

# Physicochemical Properties and Solubilization of Acid Red-27 Dye in CTABr Micellar Media: Enhanced Trapping and Interactional Investigation

Esan Olaseni Segun\* 

Department of Chemical Sciences, Adekunle Ajasin University, Akungba Akoko, Nigeria

\*Corresponding Author E-mail: [segun.olaseni@aaua.edu.ng](mailto:segun.olaseni@aaua.edu.ng)

Received: 2023-08-11, Revised: 2023-09-07, Accepted: 2023-10-21

## Abstract

This study delves into the investigation of the physicochemical characteristics and solubilization patterns of AR-27 dye within micellar environments containing the cationic surfactant CTABr, in conjunction with various electrolytes. The primary aim is to explore the augmented sequestration of AR-27 dye and its interplay with CTABr micelles through the utilization of UV-Visible Spectroscopy. The outcomes reveal a substantial enhancement in dye entrapment when electrolytes are introduced into CTABr micellar solutions compared to CTABr alone. Specifically, the partition coefficient ( $K_x$ ) for AR-27 dye in CTABr media devoid of salt stands at  $5.29 \times 10^5$ , whereas in combination with NaCl, KCl, and  $\text{NH}_4\text{Cl}$ , the  $K_x$  values escalate to  $1.46 \times 10^6$ ,  $1.84 \times 10^6$ , and  $2.57 \times 10^6$ , respectively. Furthermore, the binding constants ( $K_b$ ) for CTABr, CTABr/ $\text{NH}_4\text{Cl}$ , CTABr/KCl, and CTABr/NaCl are determined as  $4.8 \times 10^3$ ,  $4.4 \times 10^4$ ,  $2.6 \times 10^4$ , and  $1.84 \times 10^4 \text{ dm}^3/\text{mol}$ , respectively. Lower Gibbs free energy values indicate a deeper penetration of dye molecules into the micelles. To sum up, this research underscores the pivotal role of incorporating electrolytes into CTABr micellar media in augmenting the sequestration of AR-27 dye. These findings offer valuable insights into the physicochemical attributes and solubilization dynamics of AR-27 dye within CTABr micellar environments, enhancing our comprehension of the interactions between the dye and micellar structures.

**Keywords:** Solubilization, Self-aggregation, Acid Red-27, Hydrophobic, Critical micelle concentration, Partition constant.

## Introduction

Acid Red 27 (AR-27) is an anionic dye with high water solubility that finds extensive application in the coloring of textiles, paper, carpet, wood, leather, and other materials [1-2]. However, a significant concern arises from the discharge of excess AR-27 dye into

wastewater, which not only poses environmental risks but also presents numerous detrimental health effects.

The consequences of exposure to these dyes encompass eye irritation, tumor formation, birth defects, respiratory problems, and elevated levels of genotoxicity, cytotoxicity, cytostaticity, mutagenicity, and carcinogenicity.

To protect the environment and ensure the safety of individuals, it becomes imperative to implement effective strategies for the removal of AR-27 from wastewater before its discharge. By addressing the challenge of AR-27 contamination, we can mitigate the adverse impacts associated with its presence and prevent its entry into the environment, thus safeguarding both ecological balance and human well-being.

Several physicochemical techniques have been explored for dye decolorization and removal, including adsorption, chemical flocculation and coagulation, ultra-filtration, membrane-based separation, froth flotation, ion exchange, and reverse osmosis. However, these approaches have proven unsuitable for large-scale treatment of industrial effluents due to their high costs, poor efficiency, and issues with residual waste, secondary contamination, and limited applicability across a wide range of synthetic dyes [3-4].

Amphiphilic chemicals known as surfactants play a crucial role in enhancing the solubility of compounds used as excipients and additives. These surfactants have proven useful both in nature and various industries. At very low concentrations, they adsorb at the water-air interface and form self-aggregating micelles when the critical micelle concentration (CMC) is reached [8, 9]. Determining the CMC can be achieved through various methods, such as UV-Visible spectroscopy, conductometry, surface tension, and fluorometry [7-13].

Micelles, characterized by isotropic motifs composed of surfactants with a hydrophilic head and a hydrophobic tail, have a profound impact on the solubilization of less soluble or scarcely soluble compounds in aqueous environments [14]. The interactions between dyes and surfactants depend on

the type and chemical structures of the involved substances [13, 15-16]. Intermolecular forces such as Van der Waals forces, hydrophobic and electrostatic interactions, hydrogen bonds, and  $\pi$ -stacking predominantly govern these partnerships [17-20].

The strength of these interactions can be measured through parameters such as binding constants ( $K_b$ ), partition coefficients ( $K_x$ ), and changes in thermodynamic properties [21-22]. Micellar media's ability to solubilize and detergent is intimately connected to micellization. Apart from aiding colorant adsorption and fixation on substrates, surfactants also facilitate the removal of weakly attached dye molecules through solubilization, making them an attractive option for increasing the solubility, dispersion, and stability of dye solutions, especially in the textile industry.

In this study, we focus on the AR-27 dye due to its extensive use as a food colorant and in numerous pharmaceutical formulations, as well as the scarcity of investigations into its interactions with surfactants [23-24]. In addition, we explore the influence of inorganic salts on the solubilization of water-insoluble dyes in the presence of ionic surfactants. Although limited research has been conducted in this area, understanding the underlying mechanisms and optimizing the micellar media application has the potential to revolutionize the spontaneous dissolution of dyes [25-30]. By investigating the ideal micellar media and conditions for dye solubilization, this study aims to contribute to the advancement of dye decolorization techniques and pave the way for effective and sustainable solutions for the treatment of industrial effluents. [Figure 1](#) displays molecular structures of Acid Red -27 and Cetyltrimethylammonium bromide.

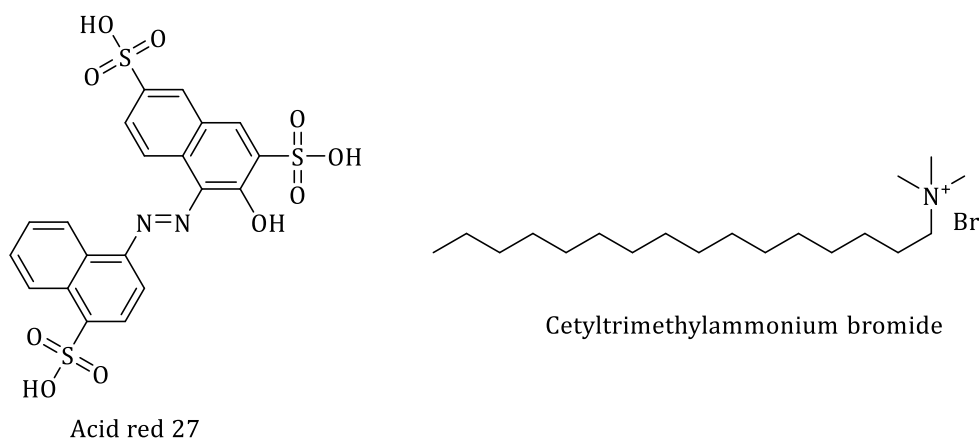


**Figure 1** Molecular structure of Acid Red 27 and Cetyltrimethylammonium bromide

## Material and Method

### Materials

Acid Red-27 (AR-27) dye, Cetyltrimethyl ammonium bromide (CTABr) was purchased from Sigma Aldrich Chemical (USA). Sodium Chloride (NaCl) (purity 99.5%), KCl (purity of 98.5%), and  $\text{NH}_4\text{Cl}$  (purity of 99%) were purchased from Horse Pharmaceuticals Ltd., located in Bangladesh. All preparations employed distilled deionized water with a specific conductivity ( $\kappa$ ) of less than  $2.0 \text{ S cm}^{-1}$ . The solution of AR-27 was used to dissolve surfactants and was diluted further to prepare a series of solutions from pre-micellar to post-micellar concentration ranges. The dye used in the present study obeys Beer's law in the employed concentration range.

### Method

The behavior of the dye and surfactant system was investigated using a spectrophotometric method. A UV-1902PC spectrophotometer equipped with a quartz cuvette, which had a path length of 1 cm, was utilized for the analysis. To control the temperature within the desired range, a thermostat cell holder was employed. After preparing the stock solution of AR-27 dye and CTABr, the absorbance of the dye

solution was measured as a function of increasing surfactant concentration at the wavelength of maximum absorbance, while maintaining a fixed concentration of the electrolyte. The measurements were performed in quartz cuvettes. Both simple and differential UV-Visible absorption measurements were conducted at a precise temperature of 298 K, controlled within a 0.5 K precision. For differential spectroscopic analysis, the reference cell contained aqueous dye solutions, while distilled water served as the reference for simple absorption measurements. The sample cell contained the micellar dye solutions in a single medium. To ensure homogenization and equilibrium, all samples were left undisturbed overnight before taking measurements [31-32].

### Preparation of stock solutions and their serial dilution

The stock solutions of the dyes, with a concentration of 0.03 mM, were initially prepared in distilled water. To prepare a single solution, concentrated CTABr solution was then diluted, maintaining the highest post-micellar concentration. Secondary solutions were subsequently prepared within the highest post-micellar concentration of CTABr, and a series of serial dilutions was performed to generate solutions spanning the range

from post-micellar to pre-micellar concentrations. To achieve this, a fixed concentration range of CTABr from 0.1 mM to 2 mM was employed, with an increment of 0.01 mM. This concentration range was utilized to investigate the solubilization of the AR-27 dye, while varying the CTABr concentration.

#### Calculation of Partition and Binding Parameters

Partitioning of dye molecules between aqueous and micellar media is governed by partition law. The partition coefficient is determined by differential absorbance method reported by Kawamura *et al.* [33].

$$\frac{1}{\Delta A} = \frac{1}{K_c \Delta A_\infty (C_d + C_s^{mo})} + \frac{1}{\Delta A_\infty} \quad (1)$$

Where,  $C_d$  is the concentration of additive (dye) in  $\text{mol}\cdot\text{dm}^{-3}$ ,  $C_s^{mo}$  represents  $C_s - \text{CMC}_0$ , in the same units. Here,  $\text{CMC}_0$  is the CMC of surfactants in the absence of dye and  $C_s$  is the total surfactant concentration in  $\text{mol}\cdot\text{dm}^{-3}$ .  $\Delta A$  is differential absorbance and  $\Delta A_\infty$  represents its value at infinity.  $K_c$  is the partition constant having value in  $\text{dm}^3/\text{mol}$ . The dimensionless quantity partition coefficient,  $K_x$  is obtained as  $K_x = K_c n_w$ , where  $n_w$  is number of moles of water per  $\text{dm}^3$  [34-35]

The value of free energy change for the transfer of additive from solvent to micellar phase was calculated using the following relation.

$$\Delta G_p = -RT \ln K_x \quad (2)$$

Where,  $R$ ,  $T$ , and  $K_x$  represent general gas constant, absolute temperature and partition coefficient respectively. Later, the binding constant was calculated using the following quantitative approach;

$$\frac{C_s \cdot C_d}{\Delta A} = \frac{C_s}{\Delta \epsilon l} + \frac{1}{K_b \Delta \epsilon l} \quad (3)$$

Where,  $C_d$  represents the concentration of additive, while  $C_s$  indicates the surfactant concentration. In addition,  $\Delta A$  represents differential absorbance,  $\Delta \epsilon$  is the difference of absorption coefficient;  $l$  is the path length, while  $K_b$  stands for the binding constant [36-39].

The value of free energy change of binding was calculated using the following relation:

$$\Delta G_b = -RT \ln K_b \quad (4)$$

## Results and Discussion

#### Partitioning of AR-27 in CTAB micelles in the absence and presence of electrolyte

The UV-Visible spectrum of Acid Red 27 (AR-27) with and without electrolyte plus Cetyltrimethylammonium bromide (CTABr) was analyzed in this study, as depicted in Figure 2.

The peak at 520 nm, corresponding to the maximum absorption, was selected for further investigation. The observed increase in absorbance in the CTABr presence indicated an interaction between the dye and surfactant. This increase can be attributed to the transfer of dye molecules from the polar water phase to the non-polar core of the CTABr micelles, resulting in a reduction in absorbance in the dye-containing solution. The interaction between AR-27 and CTABr is facilitated by electrostatic and hydrophobic interactions. The anionic dye molecules are able to fit inside the cationic CTABr micelles. The increase in absorbance with increasing CTABr concentration, as shown in Figure 3, also suggests the integration of a large number of dye molecules into the surfactant micelles. The critical micelle concentration (CMC) of CTABr is found to be reduced from 0.90 mM to 0.65 mM in the presence of solubilized dye.

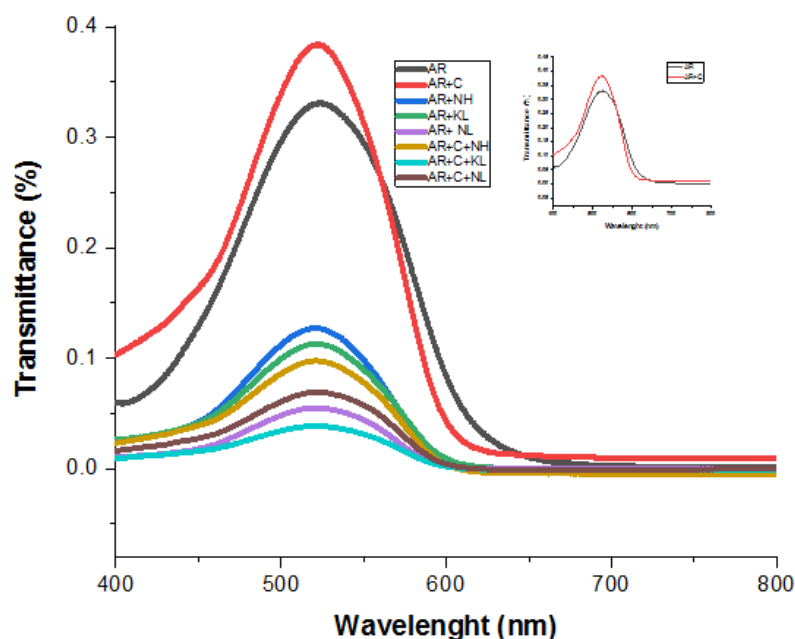


**Figure 2** (a) UV-Visible absorption spectra of AR-23 in the absence and presence of CTAB and (b) Plot of simple absorbance of AR-23 as a function of CTAB concentration

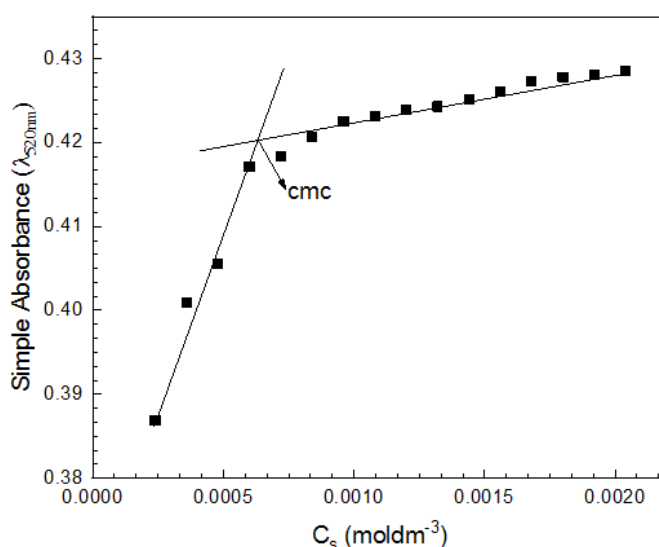


**Figure 3** Plot of simple absorbance of AR-27 as a function of CTAB concentration

This reduction can be attributed to two main mechanisms: (i) an increase in entropy upon mixing the surfactant with solubilized dye in a micelle and (ii) a decrease in the electrical work of micellization due to a decrease in repulsion between surfactant heads caused by the presence of solubilized

dye. These factors allow the dye to entice surfactant monomers to interact with each other and initiate micellization prior to reach the CMC. The experimental results for the solubilization parameters of the AR-27 dye in the presence of CTABr and electrolyte media are presented in [Tables 1-4](#).

**Table 1** Concentration of surfactant,  $c_s$ , critical micelle concentration of pure surfactant,  $cmc_o$ , and analytical concentration of surfactant, and  $C_s^{mo}$  for calculation of binding and partitioning parameters for AR-27/CTABr system

$C_s(mM)$	$1/\Delta A$	$CMC_o(mM)$	$C_s^{mo}(mM)$	$1/(C_d + C_s^{mo})(dm^3.mol^{-1})$
2.28	16.78	0.9	13.8	712.3
2.16	17.39	0.9	12.6	778.8
2.04	17.82	0.9	11.4	859.1
1.92	17.92	0.9	10.2	957.7
1.80	18.15	0.9	9.0	1082.3
1.68	18.88	0.9	7.8	1243.8
1.56	18.21	0.9	6.6	1461.9
1.44	20.92	0.9	5.4	1773.1
1.32	22.17	0.9	4.2	2252.3

**Table 2** Concentration of surfactant,  $c_s$ , critical micelle concentration of pure surfactant,  $cmc_o$ , and analytical concentration of surfactant, and  $C_s^{mo}$  for calculation of binding and partitioning parameters for AR-27/CTABr/ $NH_4Cl$  system

$C_s(mM)$	$1/\Delta A$	$CMC_o(mM)$	$C_s^{mo}(mM)$	$1/(C_d + C_s^{mo})(dm^3.mol^{-1})$
2.28	2.29	9.0	13.8	712.3
2.16	2.30	9.0	12.6	778.8
2.04	2.31	9.0	11.4	859.1
1.92	2.32	9.0	10.2	957.7
1.80	2.33	9.0	9.0	1082.3
1.68	2.34	9.0	7.8	1243.8
1.56	2.36	9.0	6.6	1461.9
1.44	2.38	9.0	5.4	1773.1
1.32	2.42	9.0	4.2	2252.3

**Table 3** Concentration of surfactant,  $c_s$ , critical micelle concentration of pure surfactant,  $cmc_o$ , and analytical concentration of surfactant, and  $C_s^{mo}$  for calculation of binding and partitioning parameters for AR-27/CTABr/KCl system

$C_s(mM)$	$1/\Delta A$	$CMC_o(mM)$	$C_s^{mo}(mM)$	$1/(C_d + C_s^{mo})(dm^3.mol^{-1})$
2.28	2.36	0.9	13.8	712.3
2.16	2.41	0.9	12.6	778.8
2.04	2.42	0.9	11.4	859.1
1.92	2.44	0.9	10.2	957.7
1.80	2.45	0.9	9.0	1082.3
1.68	2.46	0.9	7.8	1243.8
1.56	2.47	0.9	6.6	1461.9
1.44	2.48	0.9	5.4	1773.1
1.32	2.51	0.9	4.2	2252.3

This table provides detailed information about the solubilization behavior of the dye under different conditions. The partition coefficient ( $K_x$ ) was employed to assess the solubility of the dye molecules in the CTABr micellar

system. As listed in Table 5, a higher partition coefficient indicates that the dye molecules have moved farther from the bulk solution and are concentrated near the palisade region of the micelles.

**Table 4** Concentration of surfactant,  $c_s$ , critical micelle concentration of pure surfactant,  $cmc_o$ , and analytical concentration of surfactant, and  $C_s^{mo}$  for calculation of binding and partitioning parameters for AR-27/CTABr/NaCl system

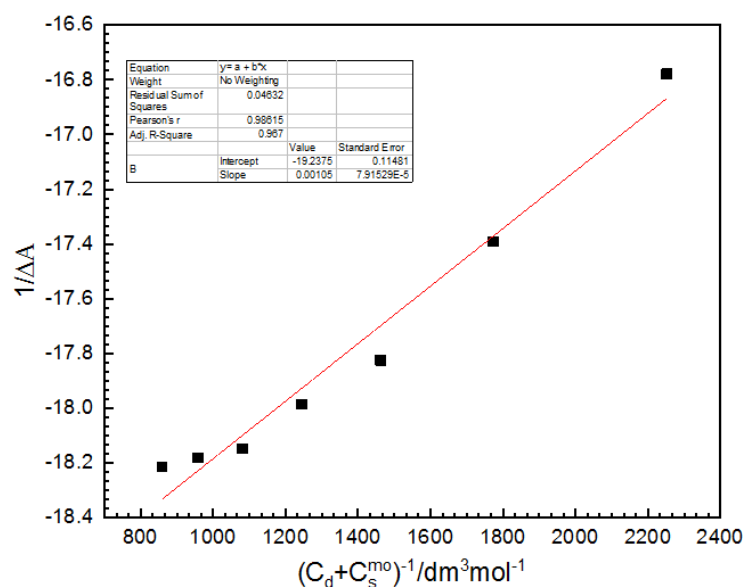
$C_s (mM)$	$1/\Delta A$	$CMC_o (mM)$	$C_s^{mo} (mM)$	$1/(C_d + C_s^{mo})(dm^3 \cdot mol^{-1})$
2.28	2.31	0.9	13.8	712.3
2.16	2.36	0.9	12.6	778.8
2.04	2.41	0.9	11.4	859.1
1.92	2.42	0.9	10.2	957.7
1.80	2.43	0.9	9.0	1082.3
1.68	2.44	0.9	7.8	1243.8
1.56	2.45	0.9	6.6	1461.9
1.44	2.46	0.9	5.4	1773.1
1.32	2.48	0.9	4.2	2252.3

**Table 5** Partition coefficient  $K_x$ , free energy of partition  $\Delta G_p$ , binding constant  $K_b$  and free energy of binding  $\Delta G_b$  for AR-27/CTABr, AR-27/CTAB /NH<sub>4</sub>Cl, AR-27/CTABr/KCl and AR-27/CTABr/NaCl systems

System	$10^{-5} \times K_x$	$\Delta G_p / KJmol^{-1}$	$10^{-3} \times K_b \cdot dm^3 \cdot mol^{-1}$	$\Delta G_b / KJmol^{-1}$
AR-27/CTABr	5.29	-35.18	4.80	-21.01
AR-27/CTABr/NH <sub>4</sub> Cl	25.68	-38.38	44.00	-26.53
AR-27/CTABr/KCl	18.36	-35.75	26.00	-25.20
AR-27/CTABr/NaCl	14.67	-36.58	18.40	-24.34

However, the precise location and position of the dye molecules within the micelles are not fixed due to the dynamic nature of the solubilization process. Lower partition coefficient values suggest that the dye molecules are

trapped and deeply absorbed in the center of the micelles. Figures 4 and 5 demonstrate the partitioning plot and binding constant of AR-27 in CTABr micellar medium, respectively.

**Figure 4** Relationship between  $(c_d + c_s^{mo})^{-1}$  and  $(\Delta A)^{-1}$  for calculation of  $K_x$  for the AR-27/CTABr system

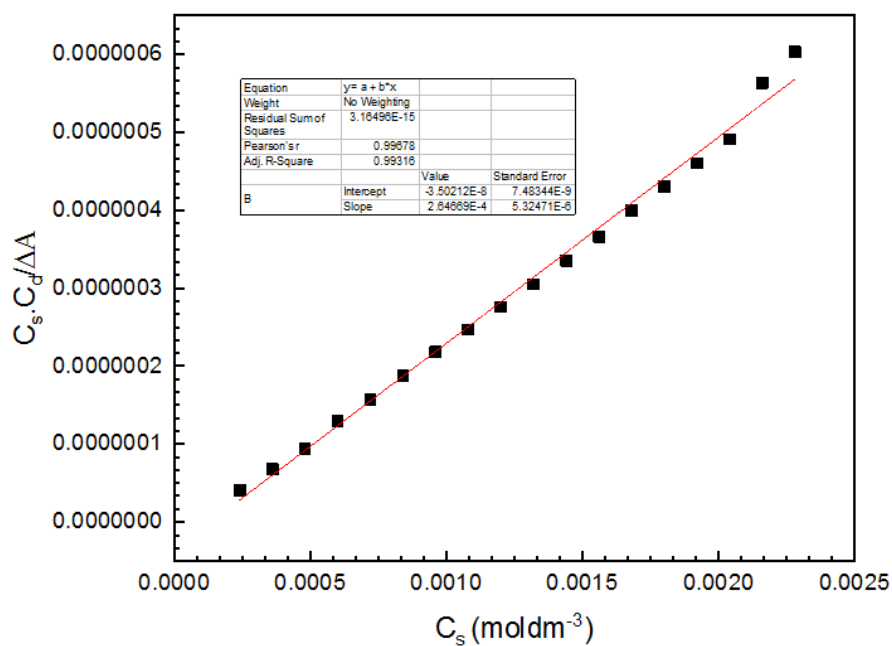


**Figure 5** Relationship between  $c_s$  and  $c_s \cdot c_d / \Delta A$  for calculation of  $K_b$  for the AR-27/CTABr system

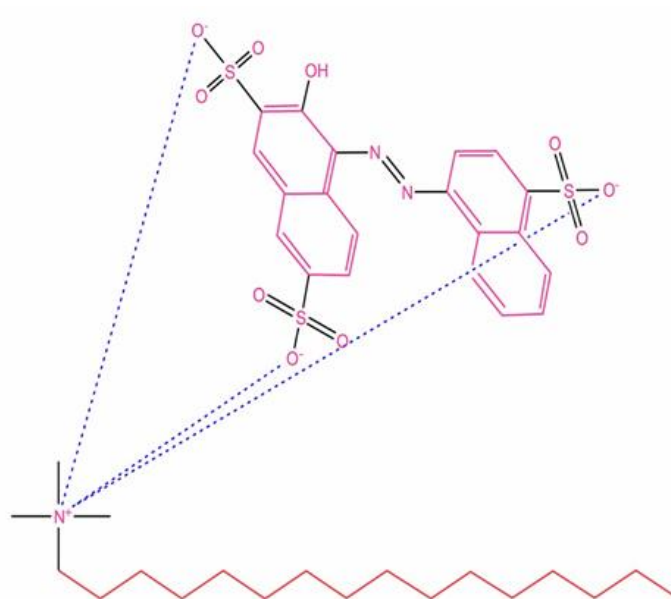


**Figure 6** Binding of AR-27 with CTABr

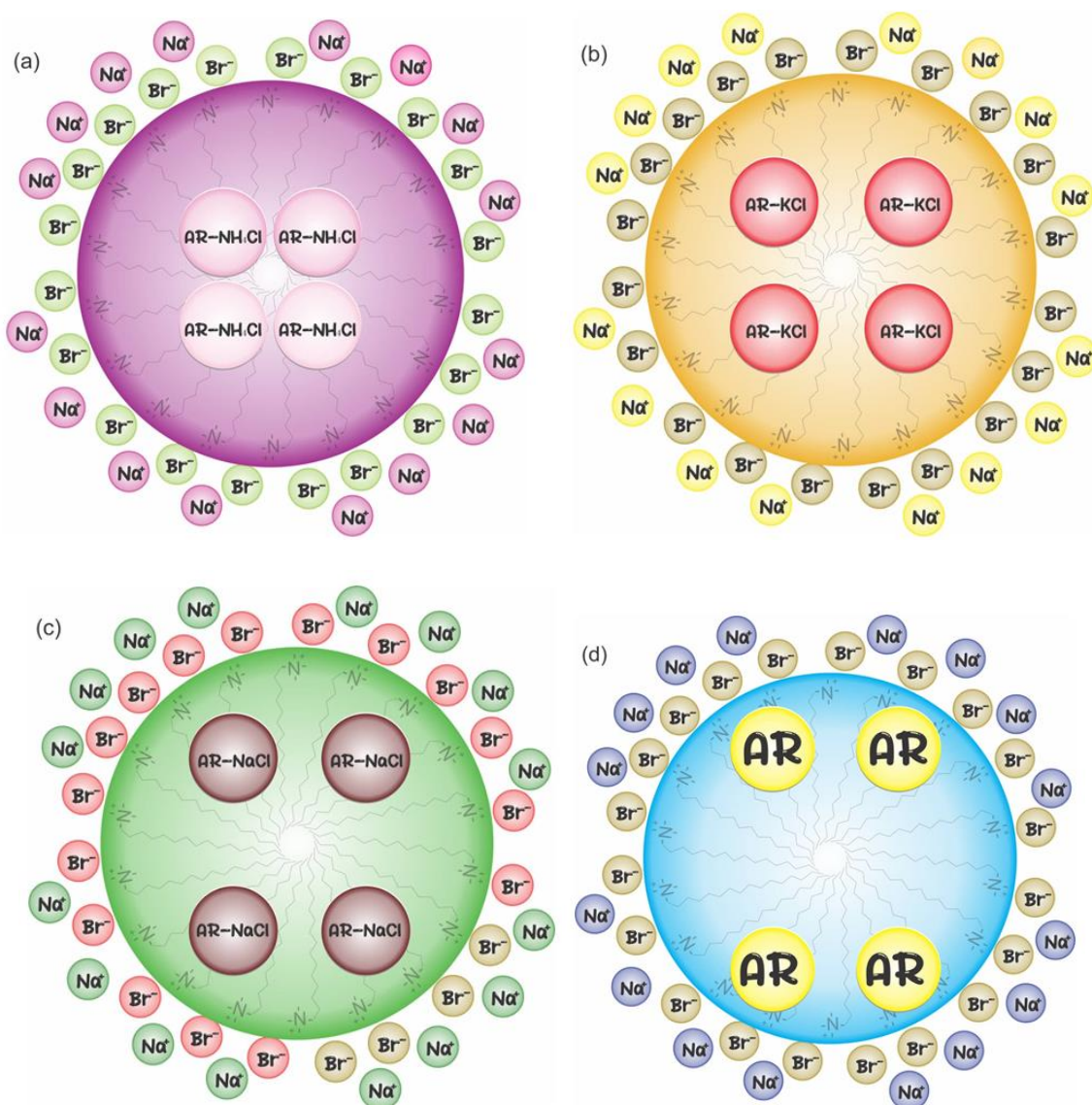


**Figure 7** Partitioning and Loci of AR-27 dye molecule in CTABr micellar media (a) AR-27 in CTABr +  $\text{NH}_4\text{Cl}$ , (b) AR-27 in CTABr +  $\text{KCl}$ , (c) AR-27 in CTABr +  $\text{NaCl}$ , and (d) AR-27 in CTABr +  $\text{H}_2\text{O}$

Equation (1) was found to provide a more accurate representation at higher CTABr concentrations, showing a linear trend. To determine the values of the  $K_c$  and  $K_x$ , a location with high CTABr concentration levels, where the  $1/(\text{C}_a + \text{C}_s^{\text{mo}})$  values were lower was chosen [33]. The dye molecules are soluble in the outer region of the micelle and are susceptible to lateral pressure, which tends to push them towards the center of the micelle. The attraction between the

anionic dye and cationic surfactant leads to the dye molecules being pushed close to the surface of the palisade layer, resulting in a high partition coefficient value. The partition coefficient for AR-27 is relatively low without electrolytes, as presented in Table 1, indicating that the dye molecules penetrate deeply into the micelle core while in the presence of electrolyte, solvatochromism occur [33], meaning that the dye's entry into the micelle's palisade layer is observed

where there is ample space, as evidently shown in [Figure 7b](#). Hence, higher partition coefficient ( $K_x$ ) is observed [40-45]. Electrolytes can have a dual effect on the solubilization of dyes. They can increase solubility by reducing aggregation, weakening electrostatic repulsions, and facilitating micelle formation, all of which contribute to higher partition coefficients ( $K_x$ ). However, in the absence of electrolyte, deep dye penetration into the micelle is hindered by the attraction between opposite charges [33]. The initial drop in absorbance may be a result of dye molecules self-aggregating with the assistance of surfactants, reducing the repulsion between dye molecules. The subsequent rise in absorbance may be attributed to dye molecules adhering to the surface of oppositely charged CTABr materials [46].

#### *Effect of electrolyte on the binding behavior between AR-27 and CTABr*

The presence of electrolytes plays a significant role in influencing the binding behavior between Acid Red 23 (AR-27) and Cetyltrimethylammonium bromide (CTABr). In comparison to the aqueous medium, the binding constants of the dye-surfactant complex are notably higher when electrolytes are present, consistent with prior research [47]. Table 1 provides a summary of the binding constant values for the dye-surfactant complex both with and without electrolytes. The increased binding strength in the presence of electrolytes such as  $\text{NH}_4\text{Cl}$ ,  $\text{KCl}$ , and  $\text{NaCl}$  is evident from the higher binding constant values [48]. The electrolytes introduction leads to an increase in binding constant due to the following reasons:

(1) Clustering of water molecules occurs due to the electrical attraction between charged ions and their electric dipole moments. This, in turn, results in a decrease in the surfactant's solubility, a

phenomenon known as the salting-out effect. As a result, the dye molecule gains better access to the surfactant molecules, leading to an increase in the binding constant.

(2) The presence of surface charges in the electrolyte causes particles to condense into a smaller volume, increasing the accessibility of the dye molecule to the surfactant and creating a stronger bond.

Table 1 illustrates that at lower electrolyte concentrations (0.1 mM), specific electrolyte cations induce an increase in binding constants in the following order: sodium ion > ammonium ion > potassium ion. This phenomenon can be explained by considering the size of these cations. As the cation size increases from sodium ion ( $\text{Na}^+$ ) to ammonium ion ( $\text{NH}_4^+$ ) to potassium ion ( $\text{K}^+$ ), the effective charge density of the cation decreases. This occurs because the charge is distributed over a larger volume, resulting in an increase in the binding constant in the specified order. It's worth noting that the sodium ion is smaller than both the potassium ion and ammonium ions, and ammonium ions have lower hydration properties compared to other ions. Consequently, the charges of the ammonium ion and potassium ions are less shielded than those of the sodium ion. This leads to a decrease in the formation of ion-pair complexes in the specified order, contributing to an increase in the binding constant. Ion-pair complex formation primarily involves electrostatic attractions between oppositely charged ions (cation and anion). Larger cations, with their more diffuse charge distribution, are less effective at forming strong electrostatic interactions with anions compared to smaller cations. The decrease in ion-pair formation, combined with improved solvent polarization associated with larger cations, results in an increase in

the binding constant, indicating a stronger and more stable interaction between the cation and anion.

## Conclusion

In conclusion, our study employed UV-Visible spectroscopy in the presence of electrolytes to investigate the interactions and solubilization behavior of AR- 27 dyes in CTABr micellar media. Through the addition of electrolytes, we successfully improved the solubilization efficiency of the dyes by reducing the critical micelle concentration (CMC) of CTABr and enhancing the hydrophobicity of the micellar system. The spectroscopic analysis utilizing various parameters, such as the binding constant ( $K_b$ ), Gibbs free energy of binding ( $\Delta G_b$ ), Gibbs free energy of partition ( $\Delta G_p$ ), and partition coefficient ( $K_x$ ), provided valuable insights into the dye-surfactant interactions and solubilization process.

Our findings demonstrated that the micellar solution of CTABr containing electrolytes served as the most effective medium for the entrapment and encapsulation of the anionic dyes. Despite primarily occupying the palisade layer of the micelles, the dyes exhibited stronger solubilization and robust interactions with the surfactant in the electrolytes presence, as evidenced by the higher values of  $K_x$ ,  $K_b$ , and  $\Delta G_b$ . The negative values of  $\Delta G_b$  and  $\Delta G_p$  further supported the spontaneous nature of these processes. Moreover, the larger values of Gibbs free energies of binding and partition indicated the efficient entrapment of dye molecules within the palisade region of the micelles, further confirming the successful solubilization of AR- 27 dye in the CTABr micellar structure.

Overall, our study provides important insights into the solubilization and interaction mechanisms of AR- 27 dye in CTABr micellar media. The electrolytes utilization not only enhanced the

solubilization efficiency, but also shed light on the robust dye-surfactant interactions. These findings contribute to the understanding and potential improvement of dye entrapment and stability in micellar systems, opening avenues for further applications in various fields such as dyeing processes, drug delivery, and material synthesis.

## ORCID

Esan Olaseni Segun

<https://orcid.org/0000-0003-0159-0113>

## References

- Guerrero-Coronilla I, Morales-Barrera L, Cristiani-Urbina E. Kinetic, isotherm and thermodynamic studies of amaranth dye biosorption from aqueous solution onto water hyacinth leaves, *J. Environ. Manage.*; 2015 Apr 1; 152:99-108. [[Crossref](#)], [[Google Scholar](#)], [[Publisher](#)]
- Liao H, Wang Z. Adsorption removal of amaranth by nanoparticles-composed Cu2O microspheres, *J. Alloy. Compd.*; 2018 Nov 15; 769:1088-95. [[Crossref](#)], [[Google Scholar](#)], [[Publisher](#)]
- Alaoui MS, Ghanam J, Merzouki M, Penninckx MJ, Benlemlih M. Immobilisation of Pycnoporus coccineus laccase in ca alginate beads for use in the degradation of aromatic compounds present in olive oil mill wastewaters, *J. Biotechnol. Lett.*; 2013 Jun 1; 4(2):91. [[Google Scholar](#)], [[Publisher](#)]
- Munawar I, Bhatti IA, Muhammad ZU, Bhatti HN, Muhammad S. Efficiency of advanced oxidation processes for detoxification of industrial effluents, *Asian J. Chem.*; 2014; 26(14):4291-6. [[Google Scholar](#)], [[Publisher](#)]
- Dave N, Joshi T. A concise review on surfactants and its significance, *Int. J. Appl. Chem*; 2017 Sep 30; 13(3):663-72. [[Crossref](#)], [[Google Scholar](#)], [[Publisher](#)]
- Smith GA, Hand KR, inventors; Huntsman Petrochemical LLC, assignee. Enhanced solubilization using extended

chain surfactants, *United States patent US 7,467,633*; 2008 Dec 23. [[Google Scholar](#)], [[Publisher](#)]

7. Taj MB, Raheel A, Alelwani W, Hajjar D, Makki A, Alnajeebi AM, Babteen NA, Tirmizi SA, Noor S. A Swift One-Pot Solvent-Free Synthesis of Benzimidazole Derivatives and Their Metal Complexes: Hydrothermal Treatment, Enzymatic Inhibition, and Solubilization Studies, *Russ. J. Gen. Chem.*; 2020 Aug; 90:1533-43. [[Crossref](#)], [[Google Scholar](#)], [[Publisher](#)]

8. Noor S, Younas N, Rashid MA, Nazir S, Usman M, Naz T. Spectroscopic, conductometric and biological investigation of [Ni (phen) 3] F2. EtOH. MeOH. 8H2O complex in anionic micellar media, *Colloids Interface Sci. Commun.*; 2018 Nov 1; 27:26-34. [[Crossref](#)], [[Google Scholar](#)], [[Publisher](#)]

9. Noor S, Taj MB. Mixed-micellar approach for enhanced dye entrapment: a spectroscopic study, *J. Mol. Liq.*; 2021 Sep 15; 338:116701. [[Crossref](#)], [[Google Scholar](#)], [[Publisher](#)]

10. Noor S, Taj MB, Ashar A. Solubilization of cationic dye in single and mixed micellar media, *J. Mol. Liq.*; 2021 May 15; 330:115613. [[Crossref](#)], [[Google Scholar](#)], [[Publisher](#)]

11. Noor S, Rashid MA. Solubilization and thermodynamic attributes of nickel phenanthroline complex in micellar media of sodium 2-ethyl hexyl sulfate and sodium bis (2-ethyl hexyl) sulfosuccinate, *Tenside Surfactants Deterg.*; 2019 Nov 15; 56(6):490-8. [[Crossref](#)], [[Google Scholar](#)], [[Publisher](#)]

12. Taj MB, Alkahtani MD, Ali U, Raheel A, Alelwani W, Alnajeebi AM, Babteen NA, Noor S, Alshater H. New heteroleptic 3D metal complexes: synthesis,

antimicrobial and solubilization parameters, *Molecules*; 2020 Sep 16; 25(18):4252. [[Crossref](#)], [[Google Scholar](#)], [[Publisher](#)]

13. Petcu AR, Rogozea EA, Lazar CA, Olteanu NL, Meghea A, Mihaly M. Specific interactions within micelle microenvironment in different charged dye/surfactant systems, *Arabian Journal of Chemistry*; 2016 Jan 1; 9(1):9-17. [[Crossref](#)], [[Google Scholar](#)], [[Publisher](#)]

14. Taboada P, Ruso JM, Garcia M, Mosquera V. Surface properties of some amphiphilic antidepressant drugs, *Colloids Surf. A Physicochem. Eng. ASP*; 2001 Apr 1; 179(1):125-8. [[Crossref](#)], [[Google Scholar](#)], [[Publisher](#)]

15. Bielska M, Sobczyńska A, Prochaska K. Dye-surfactant interaction in aqueous solutions. *Dyes Pigm.*; 2009 Feb 1; 80(2):201-5. [[Crossref](#)], [[Google Scholar](#)], [[Publisher](#)]

16. Fazeli S, Sohrabi B, Tehrani-Bagha AR. The study of Sunset Yellow anionic dye interaction with gemini and conventional cationic surfactants in aqueous solution, *Dyes Pigm.*; 2012 Dec 1; 95(3):768-75. [[Crossref](#)], [[Google Scholar](#)], [[Publisher](#)]

17. Tehrani-Bagha AR, Singh RG, Holmberg K. Solubilization of two organic dyes by cationic ester-containing gemini surfactants, *J. Colloid Interface Sci.*; 2012 Jun 15; 376(1):112-8. [[Crossref](#)], [[Google Scholar](#)], [[Publisher](#)]

18. Tehrani-Bagha AR, Holmberg K. Solubilization of hydrophobic dyes in surfactant solutions, *Materials*; 2013 Feb 21; 6(2):580-608. [[Crossref](#)], [[Google Scholar](#)], [[Publisher](#)]

19. Rashidi-Alavijeh M, Javadian S, Gharibi H, Moradi M, Tehrani-Bagha AR, Shahir AA. Intermolecular interactions between a dye and cationic surfactants:

- effects of alkyl chain, head group, and counterion, *Colloids Surf. A Physicochem. Eng. ASP.*; 2011 May 5; 380(1-3):119-27. [[Crossref](#)], [[Google Scholar](#)], [[Publisher](#)]
20. Hussain KI, Usman M, Siddiq M, Rasool N, Bokhari TH, Ibrahim M, Rana UA, Khan SU. Application of micellar-enhanced ultrafiltration for the removal of reactive blue 19 from aqueous media, *J. Disper. Sci. Technol.*; 2015 Sep 2; 36(9):1208-15. [[Crossref](#)], [[Google Scholar](#)], [[Publisher](#)]
21. Alam MS, Ragupathy R, Mandal AB. The self-association and mixed micellization of an anionic surfactant, sodium dodecyl sulfate, and a cationic surfactant, cetyltrimethylammonium bromide: conductometric, dye solubilization, and surface tension studies, *J. Disper. Sci. Technol.*; 2016 Nov 1; 37(11):1645-54. [[Crossref](#)], [[Google Scholar](#)], [[Publisher](#)]
22. Petcu AR, Rogozea EA, Lazar CA, Olteanu NL, Meghea A, Mihaly M. Specific interactions within micelle microenvironment in different charged dye/surfactant systems, *Arab. J. Chem.*; 2016 Jan 1; 9(1):9-17. [[Crossref](#)], [[Google Scholar](#)], [[Publisher](#)]
23. Asadzadeh Shahir A, Javadian S, Razavizadeh BB, Gharibi H. Comprehensive study of tartrazine/cationic surfactant interaction, *J. Phy. Chem. B*; 2011 Dec 15; 115(49):14435-44. [[Crossref](#)], [[Google Scholar](#)], [[Publisher](#)]
24. Craven BR, Datyner A. The interaction between some acid wool dyes and nonylphenol-ethylene oxide derivatives, *JSDC*; 1963 Nov; 79(11):515-9. [[Crossref](#)], [[Google Scholar](#)], [[Publisher](#)]
25. McBain JW, Wilder AG, Merrill Jr RC. Solubilization of water-insoluble dye by colloidal electrolytes and non-ionizing detergents, *J. Phy. Chem.*; 1948 Jan; 52(1):12-22. [[Crossref](#)], [[Google Scholar](#)], [[Publisher](#)]
26. Tehrani-Bagha AR, Singh RG, Holmberg K. Solubilization of two organic dyes by anionic, cationic and nonionic surfactants, *Colloid Surf. A*; 2013 Jan 20; 417:133-9. [[Crossref](#)], [[Google Scholar](#)], [[Publisher](#)]
27. Tokiwa F. Solubilization behavior of sodium dodecylpolyoxyethylene sulfates in relation to their polyoxyethylene chain lengths, *J. Phy. Chem.*; 1968 Apr; 72(4):1214-7. [[Crossref](#)], [[Google Scholar](#)], [[Publisher](#)]
28. Abe A, Imae T, Ikeda S. Solubilization properties of aqueous solutions of alkyltrimethylammonium halides toward a water-insoluble dye, *Colloid Polym. Sci.*; 1987 Jul; 265:637-45. [[Crossref](#)], [[Google Scholar](#)], [[Publisher](#)]
29. McBain JW, Green SA. Solubilization of water-insoluble dye in soap solutions: Effects of added salts, *J. Am. Chem. Soc.*; 1946 Sep; 68(9):1731-6. [[Crossref](#)], [[Google Scholar](#)], [[Publisher](#)]
30. Ozeki S, Ikeda S. The difference in solubilization power between spherical and rodlike micelles of dodecyldimethylammonium chloride in aqueous solutions, *J. Phy. Chem.*; 1985 Nov; 89(23):5088-93. [[Crossref](#)], [[Google Scholar](#)], [[Publisher](#)]
31. Ali U, Maalik A, Taj MB, Raheel A, Qureshi AK, Imran M, Sharif M, Tirmizi SA, Noor S, Alshater H. Facile Synthesis, Solubilization Studies and anti-Inflammatory Activity of Amorphous Zinc (II) Centered Aldimine Complexes, *Rev. Roum. Chim*; 2020 Oct 1; 65(10):929-41. [[Crossref](#)], [[Google Scholar](#)], [[Publisher](#)]

32. Akhtar MN, Noor S, Taj MB, Khalid M, Imran M. Thermodynamic and solubilization properties of a polynuclear copper complex in ionic surfactants media, *J. Dispers. Sci. Technol.*; 2021 May 17; 43(1):147-55. [[Crossref](#)], [[Google Scholar](#)], [[Publisher](#)]
33. Kawamura H, Manabe M, Miyamoto Y, Fujita Y, Tokunaga S. Partition coefficients of homologous. omega-phenylalkanols between water and sodium dodecyl sulfate micelles, *J. Phys. Chem.*; 1989 Jul; 93(14):5536-40. [[Crossref](#)], [[Google Scholar](#)], [[Publisher](#)]
34. Usman M, Siddiq M. Surface and micellar properties of chloroquine diphosphate and its interactions with surfactants and human serum albumin, *J. Chem. Therm.*; 2013 Mar 1; 58:359-66. [[Crossref](#)], [[Google Scholar](#)], [[Publisher](#)]
35. Usman M, Siddiq M. Probing the micellar properties of Quinacrine 2HCl and its binding with surfactants and Human Serum Albumin, *Spectrochimica Acta Part A*; 2013 Sep 1; 113:182-90. [[Crossref](#)], [[Google Scholar](#)], [[Publisher](#)]
36. Nazar MF, Abid M, Danish M, Ashfaq M, Khan AM, Zafar MN, Mehmood S, Asif A. Impact of L-leucine on controlled release of ciprofloxacin through micellar catalyzed channels in aqueous medium, *Journal of Molecular Liquids*; 2015 Dec 1; 212:142-50. [[Crossref](#)], [[Google Scholar](#)], [[Publisher](#)]
37. Nazar MF, Mukhtar F, Chaudry S, Ashfaq M, Mehmood S, Asif A, Rana UA. Biophysical probing of antibacterial gemifloxacin assimilated in surfactant mediated molecular assemblies, *J. Mol. Liq.*; 2014 Dec 1; 200:361-8. [[Crossref](#)], [[Google Scholar](#)], [[Publisher](#)]
38. Duman O, Tunç S, Kancı B. Spectrophotometric studies on the interactions of CI Basic Red 9 and CI Acid Blue 25 with hexadecyltrimethylammonium bromide in cationic surfactant micelles, *Fluid Phase Equilibria*; 2011 Feb 15; 301(1):56-61. [[Crossref](#)], [[Google Scholar](#)], [[Publisher](#)]
39. Nazar MF, Mukhtar F, Ashfaq M, Rahman HM, Zafar MN, Sumrra SH. Physicochemical investigation of antibacterial moxifloxacin interacting with quaternary ammonium disinfectants, *Fluid Phase Equilibria*; 2015 Nov 25; 406:47-54. [[Crossref](#)], [[Google Scholar](#)], [[Publisher](#)]
40. Noor S, Taj MB, Naz I. Comparative solubilization of reactive dyes in single and mixed surfactants, *J. Dispers. Sci. Technol.*; 2022 Nov 3; 43(13):2058-68. [[Crossref](#)], [[Google Scholar](#)], [[Publisher](#)]
41. M. J. Rosen, Surfactants and Interfacial Phenomenon, fourth ed., Wiley-Interscience Publication, New York (2012). [[PDF](#)]
42. Tehrani-Bagha AR, Singh RG, Holmberg K. Solubilization of two organic dyes by cationic ester-containing gemini surfactants, *J. colloid interface. Sci.*; 2012 Jun 15; 376(1):112-8. [[Crossref](#)], [[Google Scholar](#)], [[Publisher](#)]
43. Khan AM, Shah SS. A UV-visible study of partitioning of pyrene in an anionic surfactant sodium dodecyl sulfate, *J. Dispers. Sci. Technol.*; 2008 Oct 24; 29(10):1401-7. [[Crossref](#)], [[Google Scholar](#)], [[Publisher](#)]
44. Shah SS, Ahmad R, Shah SW, Asif KM, Naeem K. Synthesis of cationic hemicyanine dyes and their interactions with ionic surfactants, *Colloids Surf. A Physicochem. Eng. Asp.*; 1998 Jun 15; 137(1-3):301-5. [[Crossref](#)], [[Google Scholar](#)], [[Publisher](#)]

45. Nazar MF, Khan AM, Shah SS. Association behavior of 3, 4-Dihydroxy-9, 10-dioxo-2-anthracenesulfonic acid sodium salt in cationic surfactant medium under different pH conditions, *J. Dispers. Sci. Technol.*; 2010 Apr 21; 31(5):596-605. [Crossref], [Google Scholar], [Publisher]
46. Nazar MF, Shah SS, Khosa MA. Interaction of azo dye with cationic surfactant under different pH conditions, *JSD*; 2010 Oct; 13:529-37. [Crossref], [Google Scholar], [Publisher]
47. Saad ST, Hoque MA, Khan MA. Spectroscopic studies of the investigation of molecular interaction between Acid Red and cetyltrimethylammonium bromide, *Chem Xpress*; 2014; 3(3):111-117. [Google Scholar], [Publisher]
48. Kasaikin VA, Zakharova JA. New approach to the removal of textile dyes from wastewaters. *J. Environ. Prot. Ecol.*; 2002; 3:249-54. [Google Scholar]

**How to cite this article:**

Esan Olaseni Segun. Physicochemical Properties and Solubilization of Acid Red-27 Dye in CTABr Micellar Media: Enhanced Trapping and Interactional Investigation. *International Journal of Advanced Biological and Biomedical Research*, 2023, 11(4), 232-246.

Link: <https://www.ijabbr.com/article 708564.html>